Stabilization of a Riderless Bicycle
A Linear-Parameter-Varying Approach

VITO CERONE, DAVIDE ANDREO, MATS LARSSON, and DIEGO REGRUTO

The bicycle provides transportation for leisure, recreation, and travel between home and work, throughout the world, in big cities as well as in small villages, supporting human mobility for more than a century. In addition, this widespread vehicle probably is the least expensive means of wheeled transportation.

The bicycle has a debatable origin. Some history books speculate about Leonardo da Vinci's 1490s drawings that seem to depict a mechanical device with two wheels. The first widely recognized early bicycle precursor, called *celerifere*, a sort of toy of the French nobility built around 1790 by Comte Mede de Sivrac of France, was a wooden scooter-like device with neither pedals nor steering. In 1817 the German Baron Karl von Drais developed the first two-wheeled vehicle. This vehicle, called the *draisine* and shown in Figure 1, has a steerable front wheel. To ride the draisine, a human had to push it forward using his feet against the ground. Not until in 1861 were rotary cranks and pedals added to the front wheel of the draisine by the French inventor Pierre Michaux. The name of this new kind of vehicle was *velocipede*, which is Latin for *fast foot*, although it was sometimes called *boneshaker* because of the uncomfortable ride due to the wooden wheels and cobblestone-covered streets of the day. Indeed, driving the velocipede, riders were able to experience the bicycle's self-balancing property, noticing that this two-wheeled vehicle can balance itself when moving fast enough.

The bicycle was continually developed during the last quarter of the 19th century and the 20th century, leading to the high-performance modern device of today. An account of bicycle evolution can be found in [1] as well as in the *Proceedings of the International Cycling History Conference*, held every year since 1990 [2].

The first qualitative analysis of bicycle balancing was developed in 1869 [3], using analogies with an inverted-pendulum model. A rigorous analysis of its dynamics was given by Whipple in 1899 [4] and Carvallo in 1900 [5], where the equations of motion linearized around the upright vertical equilibrium point are derived. This model was used to show that two-wheeled vehicles are statically unstable like an inverted pendulum but can balance themselves when rolling forward in a proper speed range. This dynamic

behavior, called self-stabilization, is the basis of the statement by Einstein that "Life is like a bicycle. To keep your balance you must keep moving."

Modeling, analysis, and control of bicycle dynamics has been an attractive area of research in the last century as well as in recent years. Although articles on bicycle modeling regularly appeared during the first half of the 20th century [6]–[9], bicycle dynamics has received renewed attention since 1970, mainly due to the development of computers and software for numerical simulation.

Bicycle dynamics has attracted the attention of the automatic control research community because of its peculiar features, such as, for example, the fact that it depends strongly on the bicycle speed and that, under certain conditions, it exhibits both open right-half plane poles and zeros [10], making the design of feedback controllers for either balancing the bicycle in the upright position or moving it along a predefined path a challenging problem. In addition, the development of the motorcycle industry in the last century has motivated researchers to develop controllers to improve handling and safety of motorcycles, exploiting the results on the analysis of the bicycle

FIGURE 1 A wooden draisine with a dragon or reptile head, displayed at Deutsches Museum Verkehrszentrum, Munich, Germany. This vehicle, patented in 1817 in Germany, is the earliest known two-wheeled vehicle resembling a bicycle. The front wheel is steerable, but rotary cranks and pedals are not present, and thus a person had to push his or her feet against the ground to ride the draisine.

dynamics. In fact, these two-wheeled vehicles share many dynamic properties, among which self-stabilization [11]–[13] is perhaps the most important.

A good deal of work on the modeling and analysis of bicycle behavior has been conducted at Delft Bicycle Dynamics Lab, leading to a benchmark model [14]–[16], obtained by linearizing the motion equations for small perturbations around the constant-speed straight-ahead upright trajectory, which can be expressed by a family of linear models parameterized by the bicycle speed. For this reason, the bicycle behavior around the upright vertical equilibrium point can be described through a linear-parameter-varying (LPV) system. This kind of system can be seen as a linear system where either the matrices of the state equations or the coefficients of the difference equation relating the input and the output signals depend on one or more scheduling variables, which are time-varying parameters whose measurements are assumed to be available. The scheduling variable of the problem addressed in this article is the bicycle speed.

Through the analysis of models of varying complexity, interesting properties of the bicycle dynamics along with the main difficulties met when controlling two-wheeled vehicles are described in [10]. To design a controller that allows the bicycle to track planar trajectories while maintaining balance, an input/output (I/O) feedback linearization approach is discussed in [17], while in [18] the design of an I/O feedback control is described for bicycles equipped with a balancer used to guarantee stability even when the speed is zero. In [17] and [18] the effectiveness of the designed controller is shown by means of simulated

FIGURE 2 Prototype of the instrumented bicycle built at ABB Corporate Research, Baden, Switzerland, in collaboration with the Dipartimento di Automatica e Informatica of Politecnico di Torino, Italy. This prototype is based on a commercial city bicycle, from which brakes, chain, crankset, and pedals are removed. The vehicle is equipped with an encoder on the rear wheel, a rate gyro, and a potentiometer measuring the bicycle speed, roll velocity, and steering angle, respectively. Furthermore, a torque-driven servomotor provides a torque on the steering axis, while a general purpose ABB AC 800PEC includes a computational unit, a data acquisition unit, and a communication unit.

examples, while fuzzy control algorithms based on fuzzy sliding-mode control theory are used in [19] and [20] to guarantee stability of a bicycle.

In this article, the LPV nature of the bicycle dynamics is exploited to design a control system that automatically balances a riderless bicycle in the upright position. More precisely, the problem is formulated as the design of an LPV state-feedback controller that guarantees stability of this two-wheeled vehicle when the speed varies within a given range and its derivative is bounded. Moreover, the performance of the designed controller is tested on the prototype depicted in Figure 2, built at ABB Corporate Research, Baden, Switzerland, in collaboration with the Dipartimento di Automatica e Informatica of Politecnico di Torino, Italy.

BICYCLE MODELING

For analysis and design purposes, we consider the bicycle model presented in [14] and [16], which consists of four rigid bodies, namely, the rear frame, the front fork with the handlebar, and the rear and front knife-edge wheels. The four bodies are interconnected by revolute hinges and, in the reference configuration, they are all symmetric relative to the bicycle longitudinal axis. The contact between the stiff nonslipping wheels and the flat level surface is modeled by holonomic constraints in the normal direction as well as by nonholonomic constraints in the longitudinal and lateral direction.

In spite of its simplicity, this model adequately describes the main dynamics of the bicycle as validated by experiment [21]. This model considers three degrees of freedom, namely, the roll angle $\phi(t)$, the steering angle $\delta(t)$, and the speed $v(t)$. The linearized equations of motion are two coupled second-order ordinary differential equations written in matrix form as

$$M\ddot{q}(t) + v(t)C_1\dot{q}(t) + (K_0 + v(t)^2 K_2)q(t) = f(t), \quad (1)$$

with

$$q(t) = \begin{bmatrix} \phi(t) \\ \delta(t) \end{bmatrix}, \quad f(t) = \begin{bmatrix} T_\phi(t) \\ T_\delta(t) \end{bmatrix},$$

where $T_\phi(t)$ is an exogenous roll-torque disturbance and $T_\delta(t)$ is the steering torque provided by the actuator on the handlebar axis. The remaining quantities are the symmetric mass matrix M, the speed-dependent damping matrix $v(t)C_1$, and the stiffness matrix, which is the sum of a constant symmetric part K_0 and a quadratically speed-dependent part $v^2 K_2$. The entries of these matrices depend on the geometric parameters of the bicycle [14], [16].

The linearized ordinary differential equation (1) is rewritten in state-space form choosing the roll angle $\phi(t)$, the steering angle $\delta(t)$, and their derivatives $\dot{\phi}(t)$ and $\dot{\delta}(t)$, respectively, as state variables. The control input $u(t)$ is the torque $T_\delta(t)$ applied to the handlebar axis. The measured

output $y(t)$ includes all of the state variables. On the basis of the above considerations and from (1), the state-space equations are

$$\dot{x}(t) = A(v(t))x(t) + Bu(t), \quad (2)$$
$$y(t) = Cx(t) + Du(t), \quad (3)$$

where

$$x(t) = \left[\phi(t)\ \delta(t)\ \dot{\phi}(t)\ \dot{\delta}(t)\right]^T, \quad u(t) = T_\delta(t), \quad y(t) = x(t). \quad (4)$$

The entries of the matrices $A(v(t))$, B, C, and D depend on the geometry as well as the physical parameters of the bicycle [14]. In particular, the numerical values of the matrices $A(v(t))$, B, C, and D for the prototype shown in Figure 2 are

$A(v) =$

$$\begin{bmatrix} 0 & 0 & 1 & 0 \\ 0 & 0 & 0 & 1 \\ 13.67 & 0.225 - 1.319\,v^2(t) & -0.164\,v(t) & -0.552\,v(t) \\ 4.857 & 10.81 - 1.125\,v^2(t) & 3.621\,v(t) & -2.388\,v(t) \end{bmatrix},$$

$$B = \begin{bmatrix} 0 \\ 0 \\ -0.339 \\ 7.457 \end{bmatrix}, \quad C = \begin{bmatrix} 1 & 0 & 0 & 0 \\ 0 & 1 & 0 & 0 \\ 0 & 0 & 1 & 0 \\ 0 & 0 & 0 & 1 \end{bmatrix}, \quad D = \begin{bmatrix} 0 \\ 0 \\ 0 \\ 0 \end{bmatrix}.$$

The dependence of $A(v(t))$ on the speed $v(t)$ qualifies the system (2)–(3) as an LPV model, that is, for each constant value of the time-varying parameter $v(t)$, (2) and (3) describe a linear time-invariant system.

The eigenvalue locations of the system (2), (3) are depicted in Figure 3 for various values of $v(t)$ in the interval $[0, 10]$ m/s. When the speed $v(t)$ is zero, the system has four real eigenvalues, $\lambda_1 = 3.23$, $\lambda_2 = -3.23$, $\lambda_3 = 3.74$, and $\lambda_4 = -3.74$, marked with circles in Figure 3. Since the eigenvalues λ_1 and λ_3 are in the open right-half plane, the bicycle is unstable when its speed is zero. As the speed increases, the eigenvalues λ_1 and λ_3 meet and become complex conjugate at $v(t) \approx 0.5$ m/s. The real part of the complex eigenvalue pair decreases as the speed increases. Following [22], this mode is called the *weave mode*, which becomes stable at the speed $v(t) = v_w \approx 3.4$ m/s. The eigenvalue λ_2 remains real and moves toward the open right-half plane with increasing speed and becomes unstable at the critical speed $v(t) = v_c \approx 4.1$ m/s. The eigenvalue λ_4 moves to the left as the speed increases. For large speed v, the eigenvalue λ_2 approaches zero. The values of v_w and v_c depend on the value of the bicycle parameters and the bicycle's geometry.

Since the plant dynamics depend strongly on the speed, it is evident that the task of controlling a riderless bicycle is a challenging problem. In Figure 4, the real
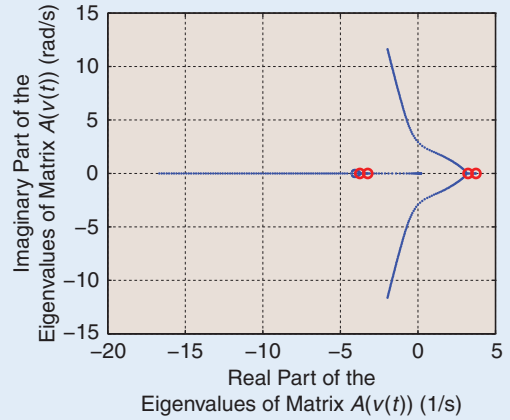

FIGURE 3 Eigenvalue trajectories for the uncontrolled bicycle for speed $v(t)$ taking values between 0 and 10 m/s. The red circles correspond to the eigenvalues of the prototype for $v(t) = 0$ m/s. For this speed the uncontrolled vehicle is unstable since two eigenvalues are located in the open right-half plane.
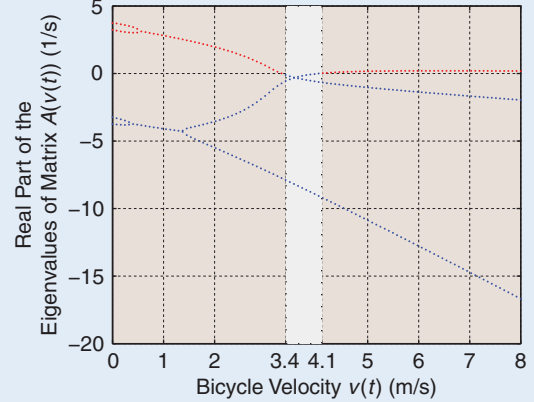

FIGURE 4 Real part of the eigenvalues of the matrix $A(v(t))$ as a function of the speed $v(t)$. The red dots denote eigenvalues with positive real part, while the blue dots denote eigenvalues with negative real part. This figure shows that the dynamic behavior of the bicycle depends on its speed. More precisely, the uncontrolled bicycle can balance itself around the vertical equilibrium point for a speed range v between about 3.4 m/s and 4.1 m/s, where the real part of each eigenvalue is negative.

part of the eigenvalues of the matrix $A(v(t))$ in (4) is reported as a function of the speed $v(t)$. It can be shown that, for constant speed values v between about 3.4 m/s and 4.1 m/s, the uncontrolled bicycle can balance itself in the vertical equilibrium since the real part of all eigenvalues of the matrix $A(v)$ are negative. As shown in [12], for speed values higher than 4.1 m/s, the unstable mode can be stabilized by applying a leaning torque as, for instance, the torque caused by a suitable rider body motion that shifts the center of gravity, as experienced in hands-free riding.

CONTROL PROBLEM FORMULATION AND SOLUTION

We consider the design of a control system to automatically balance a riderless bicycle in the upright position. This problem can be formulated as the design of a feedback controller that guarantees the stability of the LPV system described by (2) and (3) when the speed $v(t)$ is allowed to vary in the interval $[0, \gamma]$, and its derivative $\dot{v}(t)$ satisfies the constraint $|\dot{v}(t)| \leq \rho$, where γ and ρ are known constants. Since the prototype under consideration is not equipped with an active wheel traction system, during the experimental tests a human operator makes the bicycle run by pushing it for few seconds. For these experimental conditions, $\gamma = 5$ m/s and $\rho = 0.5$ m/s^2.

Since all the state variables of system (2), (3) are measured, a static state-feedback control structure is chosen. Furthermore, since the dynamics of the system to be controlled depend on the time-varying parameter $v(t)$ and a measurement of that parameter is available, an LPV controller of the form $u = K(v(t))x$ is sought that, on the basis of the measurements of $v(t)$ and $x(t)$, provides the control input $u(t)$ that guarantees stability of the closed-loop LPV system when $v(t) \in [0, \gamma]$ and $|\dot{v}(t)| \leq \rho$.

Exploiting results on LPV control discussed in "State-Feedback Stabilization of Linear-Parameter-Varying Systems," it can be shown [23] that a stabilizing state-feedback controller $K(v(t))$ exists if and only if the linear matrix inequality (LMI)

State-Feedback Stabilization of Linear-Parameter-Varying Systems

Consider the continuous-time linear-parameter-varying (LPV) dynamic system

$$\dot{x}(t) = A(p(t))x(t) + B(p(t))u(t), \tag{S1}$$
$$y(t) = C(p(t))x(t) + D(p(t))u(t), \tag{S2}$$

where $p(t) \in \mathbb{R}^m$, for all $t \in \mathbb{R}_+$, is the time-varying parameter. In addition, suppose that $p(t)$ is differentiable for all $t \in \mathbb{R}_+$. The following result provides the basis for the design of a state-feedback stabilizing controller of the form $u = K(p(t))x$. For this purpose, let $\gamma_i, \rho_i \geq 0$, $i = 1, \ldots, m$, and define the sets

$$\mathcal{P} = \{p : \mathbb{R}_+ \to \mathbb{R}^m, |p_i(t)| \leq \gamma_i, i = 1, \ldots, q, \quad t \in \mathbb{R}_+\},$$
$$\mathcal{S} = \{p : \mathbb{R}_+ \to \mathbb{R}^m, |\dot{p}_i(t)| \leq \rho_i, i = 1, \ldots, q, \quad t \in \mathbb{R}_+\}.$$

PROPOSITION 1 [23]

Assume there exists a matrix $X(p(t)) = X^\mathsf{T}(p(t)) > 0$ such that

$$X(p(t))(A(p(t)) + BK(p(t))) + (A(p(t))$$
$$+ BK(p(t)))^\mathsf{T} X(p(t)) + \sum_{i=1}^{m} \rho_i(\partial X(p(t))/\partial p_i(t)) < 0, \tag{S3}$$

for all $p(t) \in \mathcal{P} \cap \mathcal{S}$. Then the zero solution of the closed-loop system

$$\dot{x}(t) = (A(p(t)) + BK(p(t)))x(t) \tag{S4}$$

is exponentially stable for all trajectories of the time-varying parameter $p(t)$ such that $p(t) \in \mathcal{P} \cap \mathcal{S}$.

Proposition 1 states that the problem of designing a feedback controller that guarantees exponential stability of the LPV system described by (S1) and (S2) can be solved by performing a numerical search for a pair of parameter-dependent matrices $X(p(t))$ and $K(p(t))$ that satisfy the matrix inequality (S3). Unfortunately, since inequality (S3) is a nonlinear constraint on the variables $X(p(t))$ and $K(p(t))$, we are faced with a nonlinear feasibility problem. However, by means of suitable manipulations, it can be shown [23] that the existence of a pair of matrices $X(p(t))$

and $K(p(t))$ satisfying the nonconvex constraint (S3) is equivalent to the existence of the matrices

$$Y(p(t)) \doteq X^{-1}(p(t)) > 0, \tag{S5}$$
$$\overline{K}(p(t)) \doteq K(p(t))X^{-1}(p(t)), \tag{S6}$$

satisfying the linear matrix inequality (LMI)

$$A(p(t))Y(p(t)) + B\overline{K}(p(t)) + Y(p(t))A^\mathsf{T}(p(t)) + \overline{K}^\mathsf{T}(p(t))B^\mathsf{T}$$
$$- \sum_{i=1}^{m} \rho_i(\partial Y(p(t))/\partial p_i(t)) < 0. \tag{S7}$$

Solutions to LMIs can be found through efficient convex optimization tools [27].

Due to the dependence on the parameter $p(t)$, (S5) and (S7) represent parameterized linear matrix inequalities (PLMIs), which are an infinite family of LMIs that depend on one or more known parameters. As discussed in [23], the simplest approach to reducing the problem to the solution of a finite set of LMIs is parameter discretization. More precisely, the infinite-dimensional family of LMIs in (S7) can be approximately converted to a finite collection of LMIs by gridding the space of parameter values and exploiting a finite-difference approximation for the partial derivatives. The problem of solving a class of PLMI more general than the one considered here is addressed in [28], which presents a systematic approach for selecting the gridding density to guarantee global solvability of the PLMIs over all $p(t) \in \mathcal{P}$. Although the gridding approach provides approximate solutions, it leads to a collection of LMIs whose dimension grows rapidly with the number of varying parameters making it computationally cumbersome. For these reasons, alternative methods [26] provide guaranteed solutions of PLMIs. Since these methods are based on the idea of constructing a convex relaxation of the original PLMI, they are intrinsically conservative. The research challenge is thus to reduce this conservatism. Along these lines, a methodology based on sum of squares decomposition is discussed for the case of polynomial LPV systems in [26].

$$A(v(t))Y(v(t)) + B\overline{K}(v(t)) + Y(v(t))A^{\mathrm{T}}(v(t)) + \overline{K}^{\mathrm{T}}(v(t))B^{\mathrm{T}}$$
$$-\dot{v}(t)\frac{dY(v(t))}{dv} < 0 \qquad (5)$$

is satisfied, where

$$Y(v(t)) \doteq X^{-1}(v(t)) > 0, \ \overline{K}(v(t)) \doteq K(v(t))X^{-1}(v(t)), \quad (6)$$

and $X(v(t))$ is symmetric. Due to the dependence on the parameter $v(t)$, (5) qualifies as a parameterized linear matrix inequality (PLMI), which is equivalent to an infinite family of LMIs. Among various approaches for transforming (5) into a finite collection of standard LMIs, parameter discretization is exploited here. More precisely, by dividing the interval $[0, \gamma]$ into N subintervals and exploiting a forward difference approximation for the derivative, constraint (5) is approximated by the finite collection of LMIs

$$Y(jh) > 0, \quad j = 0, \dots, N-1, \qquad (7)$$

$$A(jh)Y(jh) + B\overline{K}(jh) + Y(jh)A^{\mathrm{T}}(jh) + \overline{K}^{\mathrm{T}}(jh)B^{\mathrm{T}}$$
$$\pm \rho \frac{Y(jh+h) - Y(jh)}{h} < 0, \quad j = 0, \dots, N-1, \quad (8)$$

where h is the width of the velocity subintervals.

The discretization is performed by choosing $N = 100$ and $h = 0.05$ m/s. According to [24], to guarantee a minimal damping ratio ζ and a maximal natural frequency ω_n for the eigenvalues of the matrix $A(v(t)) + BK(v(t))$, for each fixed value of $v(t) = jh$ obtained from the discretization of the interval $[0, \gamma]$, the constraints

$$\begin{bmatrix} -\dfrac{\omega_n}{\sqrt{1-\zeta^2}}Y(jh) & A(jh)Y(jh) + B(jh)\overline{K}(jh) \\ Y(jh)A(jh)^{\mathrm{T}} + \overline{K}^{\mathrm{T}}(jh)B^{\mathrm{T}} & -\dfrac{\omega_n}{\sqrt{1-\zeta^2}}Y(jh) \end{bmatrix} < 0,$$
$$j = 0, \dots, N-1, \qquad (9)$$

$$\begin{bmatrix} (A(jh)Y(jh) + B\overline{K}(jh) + Y(jh)A(jh)^{\mathrm{T}} + \overline{K}^{\mathrm{T}}(jh)B^{\mathrm{T}})\sqrt{1-\zeta^2} \\ (Y(jh)A(jh)^{\mathrm{T}} - \overline{K}^{\mathrm{T}}(jh)B^{\mathrm{T}} - A(jh)Y(jh) - B\overline{K}(jh))\zeta \end{bmatrix}$$
$$\begin{matrix} (A(jh)Y(jh) + B\overline{K}(jh) - Y(jh)A(jh)^{\mathrm{T}} - \overline{K}^{\mathrm{T}}(jh)B^{\mathrm{T}})\zeta \\ (A(jh)Y(jh) + B\overline{K}(jh) + Y(jh)A(jh)^{\mathrm{T}} + \overline{K}^{\mathrm{T}}(jh)B^{\mathrm{T}})\sqrt{1-\zeta^2} \end{matrix} < 0,$$
$$j = 0, \dots, N-1, \qquad (10)$$

are added to the design problem.

The minimal damping factor ζ is set to 0.6 to avoid underdamped oscillation in the response, while $\omega_n = 20$ rad/s is selected based on the plant model simulation, which reveals that for $\omega_n > 25$ rad/s a steering torque larger than 1.5 N-m is required, leading to saturation of the actuator mounted on the prototype.
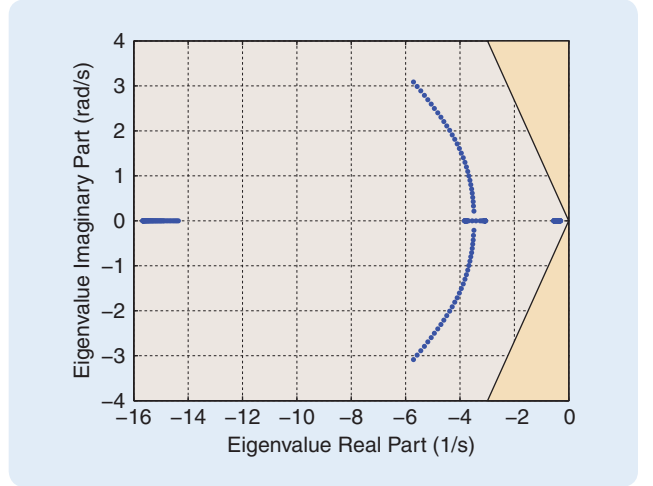

FIGURE 5 Location of the controlled bicycle eigenvalues for speed $v(t)$ in the interval 0–5 m/s. The root locus for the closed-loop system lies in the region defined by the damping ratio constraints corresponding to $\zeta \geq 0.6$.

A feasible solution over the set of LMIs described by (7)–(10) is computed using the Matlab solver SeDuMi [25]. Using the computed values of the discretized variables $Y(jh)$ and $\overline{K}(jh)$, continuous solutions $Y(v(t))$ and $\overline{K}(v(t))$ are formed by linear interpolation. Finally, the state-feedback gain matrix $K(v(t))$ is obtained from (6) as $K(v(t)) = \overline{K}(v(t))Y(v(t))^{-1}$. The locations of the closed-loop eigenvalues when $v(t)$ ranges from 0 m/s to 5 m/s are depicted in Figure 5.

Since the bicycle dynamics depend on only a single parameter, we use gridding, although this approach provides only an approximate solution and becomes computationally cumbersome when the number of varying parameters increases. For the bicycle, a fine discretization can be performed since, in the case of one parameter, the number of LMI constraints grows linearly with the number of grid points. An alternative approach for the approximate solution of the linear matrix inequality (5) in the presence of a large number of parameters is discussed in [26].

PROTOTYPE DESCRIPTION

The prototype used for the experiment is built from a commercial city bicycle whose brakes, chain, crankset, and pedals are removed. To implement the control law, the bicycle is equipped with an industrial processing platform, an actuator providing the torque on the handlebar axis, and three sensors.

Processing Platform

The processing platform is the AC 800PEC, made by ABB, which includes a computational unit, a data acquisition unit, and a communication unit. In particular, the processor module is a 64-bit IEEE floating-point RISC processor,
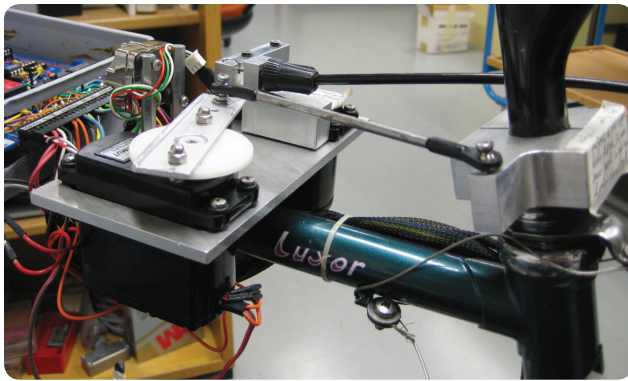
FIGURE 6 Detail of the instrumented prototype. Through a lever system, a servomotor mounted on the top tube applies a torque to the bicycle handlebar. Next to the servomotor, a rate gyro senses the angular velocity. Behind the servomotor and rate gyro is the electronic circuitry for conditioning the actuator and sensors signals.

FIGURE 7 Detail of the instrumented bicycle. The encoder on the rear wheel uses a Hall effect sensor and 36 ferrous metal plates. Calculation of the speed based on the sensor pulses is performed by the AC 800PEC processing platform.
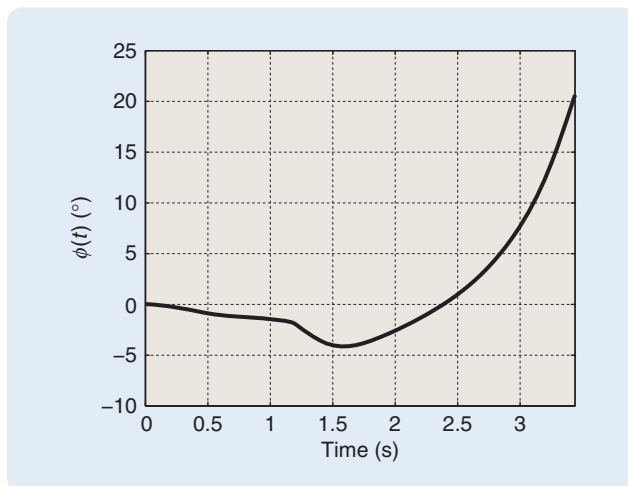
FIGURE 8 Uncontrolled bicycle. Evolution of the roll angle $\phi(t)$. The riderless prototype is pushed to a speed $v(t) = 3$ m/s and then released. For this speed the open-loop system is unstable. The roll angle reaches about 20° after 3.5 s before falling down.

400-MHz clock rate, 32-MByte SDRAM, 16-MByte flash memory, and a field programmable gate array (FPGA). Moreover, the computational unit is characterized by preemptive multitasking with three configurable basic tasks. The basic cycle time is 25 μs, while the controller update interval is 10 ms.

The input/output (I/O) module provides general purpose analog and digital interfaces, namely, three analog inputs with a 12-bit analog-to-digital converter (ADC), three analog outputs with a 12-bit digital-to-analog converter (DAC), 12 digital inputs, and 16 digital relay outputs.

A communication unit handles all internal communications between the controller and the I/O module, communication with external systems, and programming and service tools. All the main industrial interfaces are available, namely, Ethernet, CANopen, MODBUS, panel interface, and optical modules. In particular, the Ethernet interface is used to program the AC 800PEC controller and, while the software is running, to monitor and tune the software variables as well as to read the real-time data saved in the flash memory.

The AC 800PEC is programmed through the Matlab/Simulink environment and Matlab Real-Time Workshop. The controller is implemented by means of the ABB proprietary *AC PEC800 Toolbox*, containing Simulink blocks and functions compatible with the available hardware.

Actuator

To apply the torque T_δ to the steering axis of the bicycle, a Euroline Mammut servomotor is used. This servomotor, originally intended for use with model aircraft and mini-helicopters, is designed for position control. Therefore, the internal circuitry is modified to achieve a controllable torque output. The voltage-torque characteristic is determined by means of experimental measurements. The available torque is limited to ±1.5 N-m because of an internal current limitation of 2.5 A. The actuator power supply is a rechargeable 6-V NiMh battery pack providing more than 2.5 A. The torque is applied by the servomotor to the handlebar axis through the mechanical connection shown in Figure 6.

Sensors

To implement the control system, the variables to be measured are the bicycle speed $v(t)$, the roll angle $\phi(t)$, and the steering angle $\delta(t)$, as well as their time derivatives $\dot{\phi}(t)$ and $\dot{\delta}(t)$, respectively. Additionally, the bandwidth of the sensors has to be higher than the bandwidth of the measured signals. To determine the expected bandwidth and range of the quantities to be measured, the feedback-controlled system is simulated. Simulation shows that the maximum deviation of the steering angle $\delta(t)$ and roll angle $\phi(t)$ from the straight ahead position are expected

to be no larger than 15° and 40°, respectively. In addition, the maximum roll rate $\dot{\phi}(t)$ and steering rate $\dot{\delta}(t)$ remain below 100 deg/s.

The bicycle speed is measured by means of a specially built encoder, using a Hall effect sensor and 36 ferrous metal plates placed on the real wheel, as shown in Figure 7. The power supply for the encoder is taken from the AC 800PEC I/O module, and the output signal from the Hall effect sensor is digital and compatible with the AC 800PEC digital input interface. A routine for detecting the transition from zero to one is implemented, and the time T_p between two pulses, caused by the 36 plates when passing in front of the Hall sensor, is counted. Denoting by r_w the radius of the rear wheel, the bicycle speed is computed as

$$v = \frac{1}{T_p} \frac{2\pi r_w}{36}.$$

A rate gyro is used to measure the roll velocity $\dot{\phi}(t)$, while numerical integration of its output provides an estimate of the roll angle $\phi(t)$. When the controller is turned on, the initial condition of the integration is given by a pendulum connected to the bicycle frame through a linear potentiometer. More precisely, the initial value of the roll angle is selected as the mean value of the pendulum angle oscillations.

Measurement of the steering angle $\delta(t)$ is obtained by means of the servomotor built-in potentiometer giving a linear output between 1.1 V and 2 V for a ±30° range. Measurements of the steering angular velocity $\dot{\delta}(t)$ are obtained through filtered numerical differentiation of the steering angle.

EXPERIMENTAL RESULTS AND DISCUSSION
All the experimental data are collected from the time the operator releases the vehicle. Since the tests are performed in a room, the maximal value of the bicycle speed considered is about 3 m/s. Control of a riderless bicycle is more challenging at such low velocities, since the system is open-loop unstable for values of the speed $v(t)$ less than 3.4 m/s. Three different experimental tests, described below, are performed.

Uncontrolled Bicycle
In the first test the prototype is run with the control system switched off. This test is performed to show that the open-loop riderless bicycle is unstable when the speed $v(t)$ is less than 3.4 m/s. The vehicle is pushed to a speed of about 3 m/s and then released. The evolution of the roll angle $\phi(t)$ is shown in Figure 8. As expected, after a few seconds $\phi(t)$ rapidly increases, reaching a value of about 20° just before falling down.

Controlled Bicycle
In this test the prototype is pushed by the operator until the speed reaches 1.7 m/s, and then it is released. The test
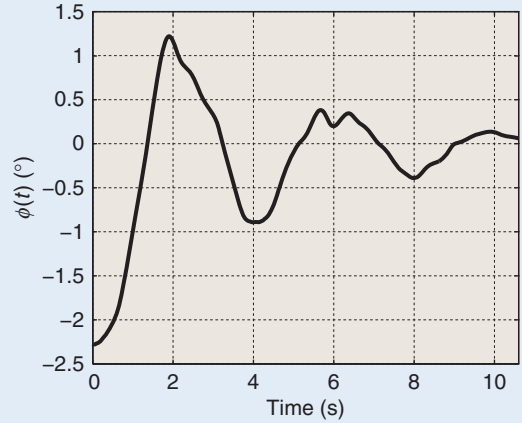
FIGURE 9 Controlled bicycle. Evolution of the roll angle $\phi(t)$. The prototype is pushed to the speed $v(t) = 1.7$ m/s. The test stops when the vehicle reaches the end of the room. After about 10 s, the amplitude of the bicycle roll angle is driven to 0.1° starting from the initial condition − 2.25°. The designed linear-parameter-varying control system thus balances the riderless bicycle in the upright position.
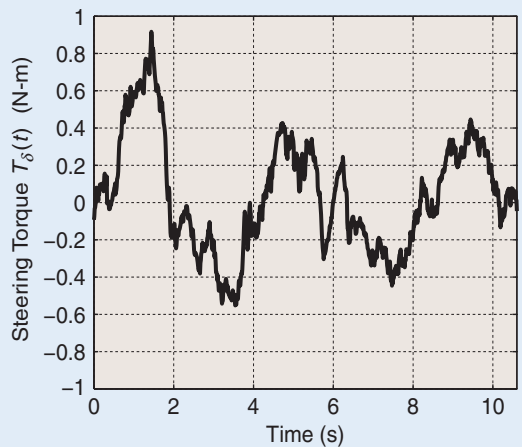
FIGURE 10 Controlled prototype. Steering torque $T_\delta(t)$ applied to the handlebar axis of the controlled bicycle. The absolute value of the amplitude of the steering torque remains less than 1.5 N-m, corresponding to the maximum torque that can be provided by the servomotor.

stops when the vehicle reaches the end of the room. The final speed is 1 m/s. The evolution of the roll angle $\phi(t)$ is depicted in Figure 9, which shows that the designed LPV control system balances the riderless bicycle in the upright position. In fact, after about 10 s, the amplitude of the roll angle $\phi(t)$ is driven to a value of about 0.1° starting from the initial condition $\phi(0) \approx -2.25°$. The steering torque $T_\delta(t)$ applied on the handlebar axis is shown in Figure 10. Figure 11 shows the bicycle speed, while Figure 12 shows the values of the state feedback gain matrix $K(v(t))$.
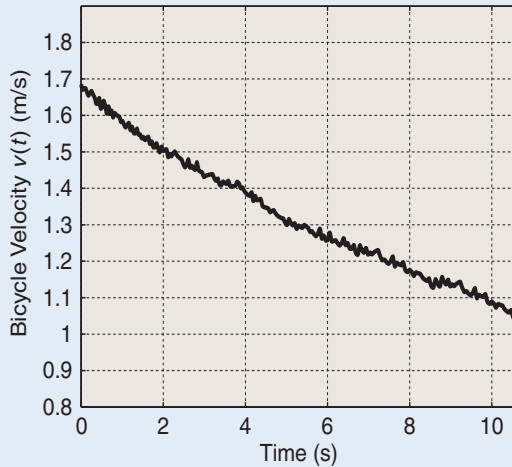
FIGURE 11 Speed $v(t)$ of the controlled riderless bicycle. Since the prototype is not equipped with actuated wheels, during the experimental tests, a human operator makes the bicycle run by pushing it for a few seconds. The bicycle speed thus decreases after the operator releases it, starting from 1.7 m/s. After 10.5 s the vehicle reaches the end of the room, and the test stops.
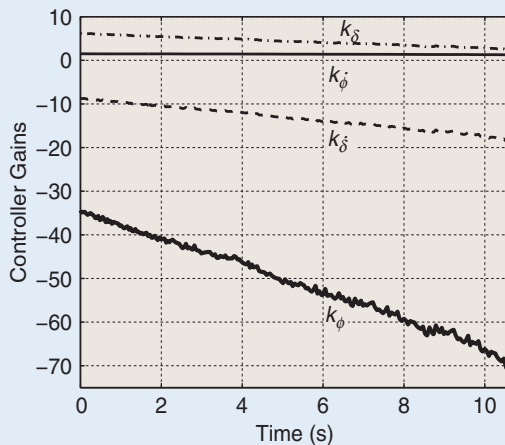

FIGURE 13 Controlled bicycle in the presence of an external impulsive roll-torque disturbance. The last plot shows the evolution of the roll angle $\phi(t)$ when the external impulsive roll-torque disturbance is about 26 N-m. The experimental data are collected from the time the roll-torque disturbance is applied to the bicycle. As a consequence of the disturbance, the roll angle reaches about −2.75° at $t \approx 0.6$ s, after which it is attenuated by the linear parameter-varying control system, decreasing to less than 0.75° around $t \approx 5.6$ s.

FIGURE 12 Controlled bicycle. Controller gains k_ϕ [N-m/rad] (solid thick), k_δ [N-m/rad] (dash-dot), $k_{\dot\phi}$ [N-m-s/rad] (solid thin), $k_{\dot\delta}$ [N-m-s/rad] (dashed). The controller gains vary with the bicycle speed $v(t)$.

FIGURE 14 Controlled bicycle in the presence of an external impulsive roll-torque disturbance. The plot shows the evolution of the steering torque $T_\delta(t)$ applied to the handlebar axis to balance the bicycle. The absolute value of $T_\delta(t)$ remains less than 1.5 N-m, which corresponds to the maximum torque provided by the servomotor.

Controlled Bicycle with External Impulsive Roll-Torque Disturbance

In this test the prototype is pushed by the operator until the speed reaches 2.1 m/s, and then it is released. The test stops when the vehicle reaches the end of the room. The final speed is about 1.6 m/s.

To evaluate the robustness of the designed control system against exogenous disturbances, such as a side wind gust, the human operator slaps the rear frame of the prototype. This input can be modeled as an impulsive roll-torque disturbance of about 26 N-m. The lateral
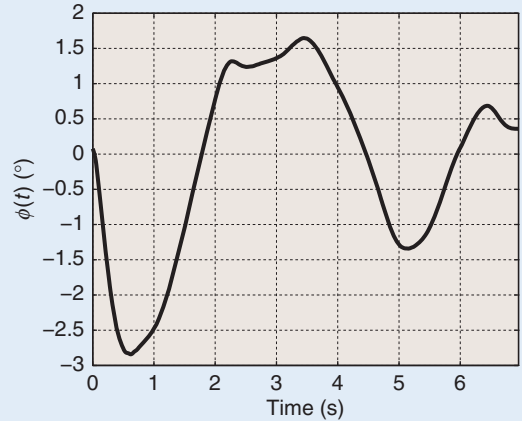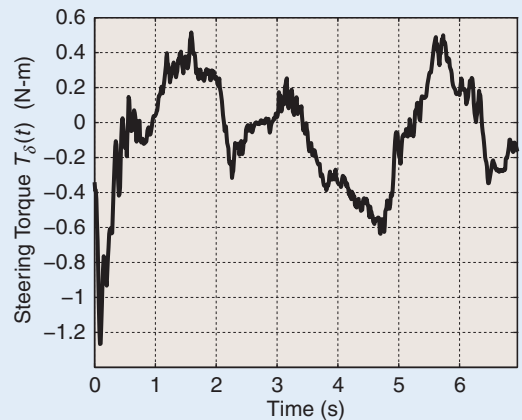
disturbance is applied just after the time the vehicle is released.

Experimental data are collected from the time the roll torque disturbance is applied to the prototype. The evolution of the roll angle $\phi(t)$ is illustrated in Figure 13, which shows that the designed LPV control system effectively balances the riderless bicycle in the upright position in the presence of the roll torque disturbance. As a consequence of the slap, the roll angle $\phi(t)$ reaches a maximum value of about −2.75° at $t \approx 0.6$ s, after which it is attenuated by the control system, decreasing to less than 0.75° around $t \approx 5.6$ s. The
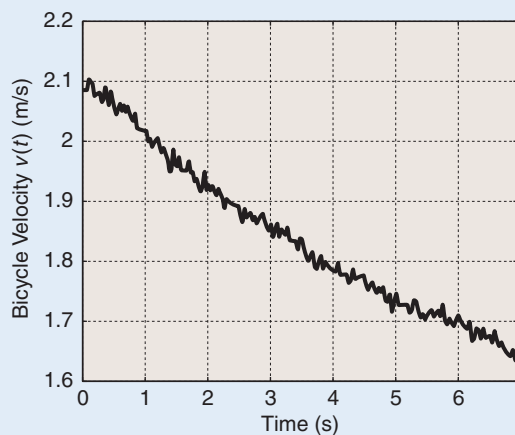
FIGURE 15 Controlled bicycle speed $v(t)$ in the presence of an external impulsive roll-torque disturbance. In this test the operator pushes the prototype until the speed reaches 2.1 m/s, then releases it, and slaps the rear frame of the bicycle. The test stops when the vehicle reaches the end of the room. The final speed is about 1.6 m/s.
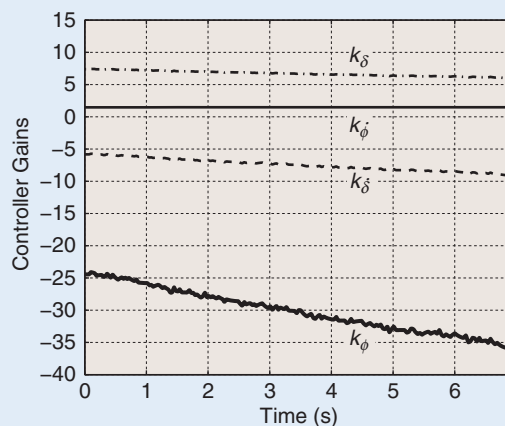

FIGURE 16 Controlled bicycle in the presence of an external impulsive roll-torque disturbance. Controller gains k_ϕ [N-m/rad] (solid thick), k_δ [N-m/rad] (dash-dot), $k_{\dot\phi}$ [N-m-s/rad] (solid thin), $k_{\dot\delta}$ [N-m-s/rad] (dashed). Although the gains k_δ, $k_{\dot\phi}$, $k_{\dot\delta}$ are approximately constant, they are expected to vary with the bicycle speed, which is the scheduling variable of the linear-parameter-varying model describing the system dynamics. The controller gain k_ϕ takes values between -25 [N-m/rad] and -35 [N-m/rad] when the bicycle speed ranges between 2.1 m/s and 1.6 m/s.

steering torque $T_\delta(t)$ applied on the handlebar axis is shown in Figure 14. Figure 15 shows the speed, while Figure 16 provides the state feedback gain matrix $K(v(t))$.

CONCLUSIONS

We considered the problem of designing a control system capable of automatically balancing a riderless bicycle in the upright position. Since the dynamics of the system to be controlled depends on the bicycle speed, an LPV state-feedback controller based on the online measurement of the system states as well as the speed is discussed. The design of the stabilizing LPV controller is formulated in terms of an LMI feasibility problem. To bound the damping and natural frequency of the closed-loop eigenvalues, suitable constraints are added to the design problem. The control system is implemented on the processing platform ABB AC 800PEC and installed on a riderless prototype equipped with suitable sensors and actuators. Experimental tests show that the designed LPV controller effectively balances the bicycle in the presence of external disturbances.

One direction for future research is the development of a more complex control system to drive the bicycle along a predefined path. The development of such a control system requires additional sensors, such as a global positioning sensor, to localize the bicycle with respect to an inertial frame as well as new actuators to make the bicycle self-propelled. Furthermore, path-following applications are likely to require the design of new control strategies.

ACKNOWLEDGMENTS

AUTHOR INFORMATION

Vito Cerone (vito.cerone@polito.it) received the Laurea in electronic engineering and the Ph.D. in system engineering from the Politecnico di Torino, Italy, in 1984 and 1989, respectively. From 1989 to 1998, he was an assistant professor with the Dipartimento di Automatica e Informatica, Politecnico di Torino, where he is currently an associate professor. He is a coauthor of *Linear Quadratic Control: An Introduction*. His research interests include system identification, parameter estimation, optimization, and control, with applications to automotive systems. He can be contacted at the Dipartimento di Automatica e Informatica, Politecnico di Torino, corso Duca degli Abruzzi 24, 10129 Torino, Italy.

Davide Andreo received the M.Sc. in mechatronics engineering in 2008 from the Politecnico di Torino, Italy. He is currently working as an R&D engineer at ABB Medium Voltage Drives in Turgi, Switzerland, where his focus is on motor control software and drive systems simulations.

Mats Larsson is a principal scientist at ABB Corporate Research in Baden, Switzerland. He has been with ABB since 2001; he is responsible for research on wide-area measurement systems and high-voltage direct current transmission and has been leading projects on substation automation and network management systems. He received the M.S. in computer science and engineering in 1993 and the Ph.D.

in industrial automation from Lund University, Sweden. Previously, he was a research assistant at Lund University and with WM-Data Ellips, a leading Swedish consultancy providing IT solutions for the energy business. He has authored or coauthored more than 40 scientific manuscripts for journals and conferences and has more than 20 patents and patent applications.

Diego Regruto received the Laurea in electronic engineering and the Ph.D. in system engineering from Politecnico di Torino in 2000 and 2004, respectively. He is currently an assistant professor at the Dipartimento di Automatica e Informatica, Politecnico di Torino. His research interests are in system identification and robust control, with application to automotive problems.

REFERENCES
[1] D. Herlihy, *Bicycle: The History*. New Haven, CT: Yale Univ. Press, 2004.
[2] *Proc. International Cycling History Conf.*, Freehold, NJ, July 29–Aug. 1, 2009.
[3] W. Rankine, "On the dynamical principles of the motion of velocipedes," *Engineer*, vol. 28, p. 79, 129, 153, 175, 1869.
[4] F. Whipple, "The stability of the motion of a bicycle," *Quart. J. Pure Appl. Math.*, vol. 30, no. 120, pp. 312–348, 1899.
[5] E. Carvallo, "Theorie du mouvement du monocycle et de la bicyclette," *Journal de l'Ecole Polytechnique*, vol. 5, pp. 119–188, 1900.
[6] A. Letov, "Stability of an automatically controlled bicycle moving on an horizontal plane," *Appl. Math. Mech.*, vol. 23, no. 4, pp. 650–655, 1959.
[7] F. Klein and A. Sommerfeld, *Über die Theorie des Kreisel*, vol. Heft IV. Leipzig, Germany: Teubner, 1910, pp. 863–884.
[8] R. Wilson-Jones, "Steering and stability of single-track vehicles," in *Proc. Automobile Division of the Institute of Mechanical Engineers*, 1951, pp. 191–199.
[9] E. Döhring, "Stability of single-track vehicles," *Institut für Fahrzeugtechnik*, Technische Hochschule Braunschweig, Forschung Ing.-Wes, vol. 21, no. 2, pp. 50–62, 1955.
[10] K. Astrom, R. Klein, and A. Lennartsson, "Bicycle dynamics and control," *IEEE Control Syst. Mag.*, vol. 25, no. 4, pp. 26–47, 2005.
[11] J. Fajans, "Steering in bicycles and motorcycles," *Amer. J. Phys.*, vol. 68, no. 7, pp. 654–659, 2000.
[12] D. Limebeer and R. Sharp, "Bicycles, motorcycles and models," *IEEE Control Syst. Mag.*, vol. 6, no. 5, pp. 34–61, 2006.
[13] R. Frezza and A. Beghi, "A virtual motorcycle driver for closed-loop simulation," *IEEE Control Syst. Mag.*, vol. 6, no. 5, pp. 34–61, 2006.
[14] A. Schwab, J. Meijaard, and J. Papadopoulos, "Benchmark results on the linearized equations of motion of an uncontrolled bicycle," *Int. J. Mech. Sci. Technol.*, vol. 19, no. 1, pp. 292–304, 2005.
[15] A. Schwab, J. Meijaard, and J. Papadopoulos, "A multibody dynamics benchmark on the equations of motion of an uncontrolled bicycle," in *Proc. 5th EUROMECH Nonlinear Dynamics Conf.* The Netherlands: Eindhoven Univ. Technol., Aug. 7–12, 2005, pp. 511–521.
[16] J. Meijaard, J. Papadopoulos, A. Ruina, and A. Schwab, "Linearized dynamics equations for the balance and steer of a bicycle: A benchmark and review," *Proc. R. Soc.*, vol. A463, pp. 1955–1982, 2007.
[17] N. Getz and J. Marsden, "Control for an autonomous bicycle," in *Proc. IEEE Int. Conf. Robotics and Automation*, 1995, pp. 1397–1402.
[18] M. Yamakita and A. Utano, "Automatic control of bicycles with a balancer," in *Proc. IEEE/ASME Conf. Advanced Intelligent Mechatronics*, Monterey, CA, 2005, pp. 1245–1250.
[19] L. Guo, Q. Liao, and S. Wei, "Design of fuzzy sliding mode controller for bicycle robot nonlinear system," in *Proc. IEEE Conf. Robotics and Biomimetics*, Kunming, China, 2006, pp. 176–180.
[20] N. Umashankar and H. Sharma, "Adaptive neuro-fuzzy controller for stabilizing autonomous bicycles," in *Proc. IEEE Conf. Robotics and Biomimetics*, Kunming, China, 2006, pp. 1652–1657.
[21] J. Kooijman, A. Schwab, and J. Meijaard, "Experimental validation of a model of an uncontrolled bicycle," *Multibody Syst. Dyn.*, vol. 19, no. 1–2, pp. 115–132, 2008.
[22] R. Sharp, "The stability and control of motorcycles," *J. Mech. Eng.*, vol. 13, no. 5, pp. 316–329, 1971.
[23] W. J. Rugh and J. S. Shamma, "Research on gain scheduling," *Automatica*, vol. 36, no. 10, pp. 1401–1425, 2000.
[24] M. Chilali and P. Gahinet, "H_∞ with pole placement constraints: an LMI approach," *IEEE Trans. Automat. Contr.*, vol. 41, no. 3, pp. 358–367, 1996.
[25] J. F. Sturm, "Using SeDuMi 1.02, a Matlab Toolbox for optimization over symmetric cones," *Optim. Methods Softw.*, vol. 11, no. 12, pp. 625–653, 1999.
[26] F. Wu and S. Prajna, "SOS-based solution approach to polynomial LPV system analysis and synthesis problems," *Int. J. Contr.*, vol. 78, no. 8, pp. 600–611, 2005.
[27] S. Boyd, L. El Ghaoui, E. Feron, and V. Balakrishnan, *Linear Matrix Inequalities in System and Control Theory*. Philadelphia, PA: SIAM, 1994.
[28] F. Wu, H. Yang, A. Packard, and G. Becker, "Induced L2-Norm control for LPV system with bounded parameter variations," *Int. J. Nonlinear Robust Contr.*, vol. 6, pp. 983–998, 1996.

» 25 YEARS AGO *(continued from page 19)*

minicomputers, the number of process computers grew from about 5000 in 1970 to about 50,000 in 1975.

REFERENCES
[12] P. E. A. Cowley, "Pilot plant puts DDC to the test," *Control Eng.*, vol. 13, pp. 53–56, 1966.
[13] R. H. Crowther, J. E. Pitrak, and E. N. Ply, "Computer control at American oil," *Chem. Eng. Progress*, vol. 57, pp. 39–43, 1961.
[17] Å. Ekström, "Integrated computer control of a paper machine-system summary," *IBM Nordic Lab.*, Lidingö, Sweden, Rep. TP 18.169.
[18] A. S. Foss, "Critique of chemical process control theory," *Amer. Inst. Chem. Eng. J.*, vol. 19, pp. 209–214, 1973.
[19] T. J. Harrison, *Minicomputers in Industrial Control*. Pittsburgh, PA: Instrument Society of America, 1978.
[21] IBM Reference Manual, 1720 Control System. Order No. A26-5512.
[23] J. M. Lane, "Digital computer control of a catalytic reforming unit," *ISA Trans.*, vol. 1, pp. 291–296, 1962.
[27] J. McMillan, "Five years in the doldrums," *Control*, pp. 512–515, 1966.
[30] J. F. Moore and N. F. Gardner, "Process control in the 1970s," *Chem. Eng.*, pp. 94–106, June 1969.
[34] T. M. Stout, "Computer control of butane isomerization," *ISA J.*, vol. 6, pp. 98–103, 1959.
[35] A. Thompson, "Operating experience with direct digital control," in *Proc. 1st IFAC/FIP Conf. Applications of Digital Computers to Process Control*, Stockholm, Sept. 1964.
[39] T. J. Williams, "Direct digital control computers—A coming revolution in process control," in *Proc. Texas A&M 19th Annu. Symp. Instrumentation for the Process Industries*, College Station, TX, Jan. 1964, pp. 70–81.
[40] T. J. Williams, "Computers and process control," *Ind. Eng. Chem.*, vol. 62, pp. 28–40, 1970.